COMPARATIVE STUDIES BETWEEN THE THERMAL DECOMPOSITION REACTIONS OF LANTHANIDE(III) OXALATES AND MALONATES.
Part I. The reaction processes of $Eu_2ox_3 \cdot 10H_2O$ and $Eu_2mal_3 \cdot 6H_2O$

KENZO NAGASE and HIROKO YOKOBAYASHI

College of General Education, Tohoku University, Kawauchi, Sendai 980 (Japan)

KAZUO MURAISHI

Department of Chemistry, Faculty of Science, Yamagata University, Yamagata 990 (Japan)

MASAE KIKUCHI

Institute for Material Research, Tohoku University, Katahira, Sendai 980 (Japan)

(Received 8 June 1990)

ABSTRACT

TG–DTA analyses of $Eu_2ox_3 \cdot 10H_2O$ and $Eu_2mal_3 \cdot 6H_2O$ [ox and mal = $(COO^-)_2$ and $CH_2(COO^-)_2$, respectively] were carried out in N_2, O_2 and CO_2 atmospheres. The products at each TG stage were determined on the basis of the IR spectra, X-ray diffractograms, evolved gas analyses and elemental analyses. In N_2, the decomposition processes of Eu_2ox_3 and Eu_2mal_3 were very similar and proceeded through the intermediate formation of Eu(II), which, in the case of Eu_2ox_3, was confirmed to be in the form of $EuCO_3$. In CO_2, on the other hand, the decomposition processes of the two salts were different; that of Eu_2ox_3 is represented as follows: $Eu_2ox_3 \rightarrow EuCO_3 \rightarrow Eu_2O_2CO_3 \rightarrow Eu_2O_3$, while that of Eu_2mal_3 may tentatively be formulated as follows: $Eu_2mal_3 \rightarrow EuCH(COO)_2 \rightarrow Eu_2O(CO_3)_2 \rightarrow Eu_2O_2CO_3 \rightarrow Eu_2O_3$.

INTRODUCTION

The present series of work was undertaken with the intention of making a comparative study between the thermal decomposition reactions of oxalates and malonates of various trivalent lanthanoid ions (Ln^{3+}). Oxalate (ox^{2-}) and malonate (mal^{2-}) ions are similar dicarboxylate ligands, but the latter has an active $-CH_2-$ group between its COO^- groups. It is of interest to know how this difference is reflected in these reactions.

There are many published studies on the thermal decomposition of Ln(III) oxalates [1a–1r]. For example, Glasner et al. [1d,1e,1g] carried out extensive studies, and reported that nearly all the oxalates decompose

without changing the oxidation state of Ln; exceptions are those of Ce, Eu and Yb, which decompose with such a change (3 to 4 with Ce, 3 to 2 with Eu and Yb). However, there are substantial disagreements among investigators as to the decomposition mechanisms and intermediate products, and Gallagher et al. [1n] even claimed that the intermediate formed from Eu_2ox_3 is not a Eu^{2+} species, but the carbonyl carbonate of Eu^{3+}, on the basis of the Mössbauer and emission spectral data.

In the present study, the thermogravimetry (TG) of Eu_2ox_3 was carried out in three different ambient atmospheres, N_2, O_2 and CO_2, and the results were compared with those for Eu_2mal_3. The thermal decomposition of Eu_2mal_3 has been only briefly studied by Azikov and Serebrennikov [2].

EXPERIMENTAL

Preparation of $Eu_2ox_3 \cdot 10H_2O$ and $Eu_2mal_3 \cdot 6H_2O$

The oxalate was prepared according to the literature [3]; Eu_2O_3 was dissolved in dilute HNO_3 and the solution was evaporated on a steam bath. The residue obtained was dissolved in water, and an almost saturated aqueous solution of H_2ox was poured into the solution at about 80°C. The precipitate which appeared was kept in contact with the mother liquor at 80°C for 24 h and then filtered off. The fine crystals obtained were washed with water and then ethanol and dried in air. The malonate was prepared from $EuCl_3$ and $Na(mal)$; an aqueous solution of $EuCl_3$ was poured into an aqueous solution of $Na(mal)$ at room temperature. The precipitate which appeared was allowed to stand overnight in contact with the mother liquor, and then washed several times with water by decantation and collected by filtration. The fine crystals obtained were washed with ethanol and then ether, and dried. The contents of Eu, C and H in the samples were—$Eu_2ox_3 \cdot 10H_2O$: Eu 41.08 (40.62), C 9.53 (9.63), H 2.42 (2.69)%; $Eu_2mal_3 \cdot 6H_2O$: Eu 41.90 (42.31), C 15.14 (15.05), H 2.78 (2.53)%. The theoretical values are given in parentheses.

Thermogravimetry (TG) and differential thermal analysis (DTA)

The TG and DTA curves were obtained with a Shinku Riko TGD-3000 differential microbalance at a heating rate of 3°C min^{-1} in streams of N_2, O_2 and CO_2 with a flow rate of 30 ml min^{-1}, and also at heating rates of 1° min^{-1} and 0.5° min^{-1} in a stream of CO_2 with the same flow rate. In the case of the CO_2 atmosphere, a heating rate of 3° min^{-1} was found to be too fast to obtain reliable data. About 70 mg of powdered sample in a platinum crucible was used for each run.

Infrared, X-ray diffraction and evolved gas analysis (EGA)

The IR spectra of the original samples and their products were obtained in the wavenumber range 4000–250 cm^{-1} by the Nujol mull method and the KBr disk method. The X-ray diffractograms were obtained by using Cu K_α radiation and a nickel filter. EGA was carried out with an activated carbon column and He carrier gas. The details of these procedures were described in a preceding paper [4].

Elemental analysis

The europium contents in the original samples were determined by titration with EDTA and Xylenol Orange in the pH range 5.1–5.6. The carbon and hydrogen contents in the original samples and their decomposition products were determined by the conventional combustion method.

RESULTS

Dehydration of $Eu_2ox_3 \cdot 10H_2O$

The TG and DTA curves for the runs in N_2, O_2 and CO_2 atmospheres are shown in Fig. 1. The first three endotherms, at 102°, 131° and 187°C, on the DTA curve in N_2 correspond to dehydration steps involving 4.5, 2 and
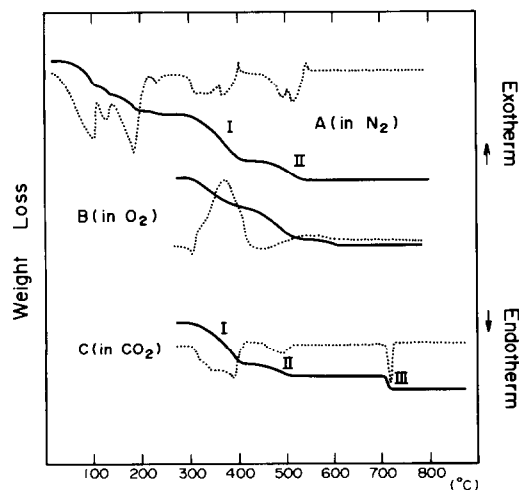

Fig. 1. TG (solid line) and DTA (dotted line) curves of $Eu_2ox_3 \cdot 10H_2O$ in various atmospheres. Heating rates used were 3° min^{-1} for the runs in N_2 and O_2, and 1° min^{-1} for the run in CO_2.
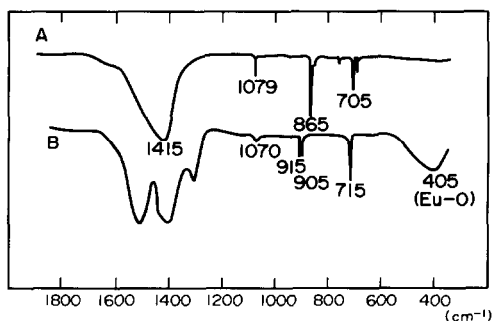
Fig. 2. Infrared spectra of the products directly after Step I in N_2 (A) and Step II in CO_2 (B) of Eu_2ox_3.

3.5 H_2O molecules, respectively. These numbers are approximate, however, because the steps overlap considerably. No effect of the ambient atmospheres was observed on the course of dehydration.

Decomposition of Eu_2ox_3 in N_2

The decomposition of the anhydrous salt, which occurs after the dehydration, was found to be strongly dependent on the ambient atmospheres. TG in N_2 (Fig. 1A) shows that the weight loss of Eu_2ox_3 begins at 299°C and continues up to 414°C (Step I). A slight TG break and some DTA peaks are observed during Step I, indicating its composite nature. The product immediately after Step I was black in color, suggesting the presence of elementary carbon. Its IR spectrum (Fig. 2A) shows the absorptions of CO_3^{2-}, and its X-ray diffractogram (Fig. 3) indicates that $EuCO_3$ [5] is its main constituent. The carbon content (6.3%) in the product was near the
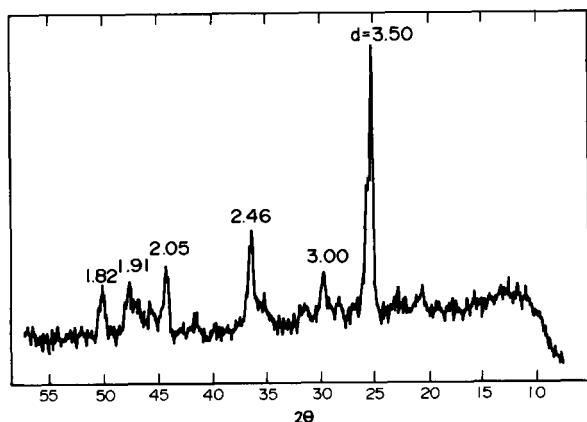

Fig. 3. X-ray diffractogram of the product directly after Step I for Eu_2ox_3 in N_2. The values of d (interplanar spacing) and their relative intensities for $EuCO_3$ are known to be 3.53 (100), 3.45 (40), 2.46 (35), 2.05 (30), 1.91 (20), 1.83 (20) and 3.02 (16) [5].
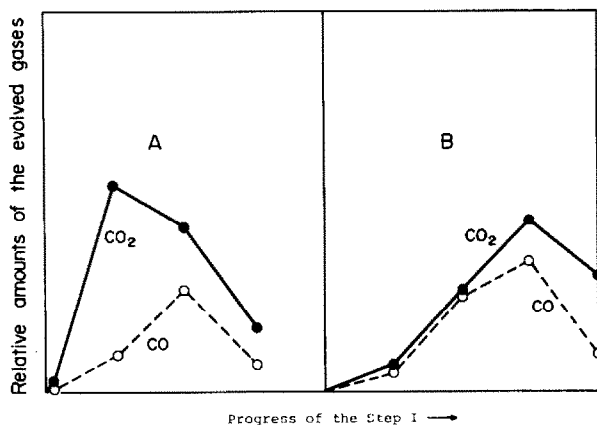
Fig. 4. Evolved gas analyses in Step I of Eu_2ox_3 (A) and Sm_2ox_3 (B) in N_2.

theoretical value (5.7%) for $EuCO_3$, but somewhat larger, possibly owing to the presence of elementary carbon referred to above. The molar ratio of CO/CO_2, determined by EGA, was 0.1 at the initial stage of Step I, and increased with the progress of the reaction (see Fig. 4A). It is known that this ratio (R) in the thermal decomposition of metal oxalates can be classified into three groups [4,6]: (1) when M^{n+} is reduced by ox^{2-}, CO_2 is predominantly evolved, and $R \ll 1$; (2) when M^{n+} is oxidized by ox^{2-}, CO is predominantly evolved, and $R \gg 1$; and (3) when the charge of M^{n+} is not changed, both CO and CO_2 are evolved, and $R \approx 1$. Although R may depend also on the shift of the disproportionation equilibrium between C, CO and CO_2 [7], it seems clear that the initial stage of Step I of Eu_2ox_3 belongs to case (1). [For comparison, the result of EGA for Sm_2ox_3 is shown in Fig. 4B, the initial stage of which belongs to the case (3)]. The observed weight loss (19.1%) of Step I was also in good agreement with the theoretical value (19.0%) for the formation of $EuCO_3$.

Step I is followed by Step II occurring in the temperature range 414–522°C. The corresponding DTA curve shows two endotherms at 495 and 515°C, respectively, indicating that Step II is composed of two reactions with different rates. The product after Step II was white, and was confirmed to be Eu_2O_3 from its X-ray diffractogram. R was about 1, and the weight loss (8.7%) was near the value for loss of $CO + CO_2$ (9.6%).

Decomposition of Eu_2ox_3 in O_2

In O_2 the weight loss of the anhydrous salt begins at 305°C, which is somewhat higher than in the case of N_2, and Eu_2O_3 was formed at 615°C without any distinct intermediate stage on the TG curve. The whole decomposition temperature range is wider by ca. 100°C than that in the case of N_2, and the DTA peaks become notably exothermic. Here the decomposi-

tion takes place in an oxidizing atmosphere, where no formation of Eu(II) is conceivable, and CO in the evolved gas will immediately burn.

Decomposition of Eu_2ox_3 in CO_2

In CO_2, the weight loss of Eu_2ox_3 begins at $302°C$ and continues up to $413°C$ with an overall weight loss of 18.1% (Step I). The product was yellowish brown, showing that only a small amount of elementary carbon was present. The TG and DTA patterns (Fig. 1C) of Step I are very similar to those of Step I in N_2, and the IR spectrum of the product is also similar to that of Fig. 2A.

Step I is followed by Step II, with a weight loss of 4.8% in the temperature range $413-506°C$. The product was white, and its IR spectrum (Fig. 2B) showed an absorption around 400 cm^{-1}, which may be ascribed to an Eu–O bond [8], in addition to CO_3^{2-} absorptions. Its carbon content (3.01%) was in good agreement with the theoretical value (3.03%) for $Eu_2O_2CO_3$ [11,1n,9]. The observed weight loss (4.8%) is somewhat higher than the loss of CO (3.7%) from $2EuCO_3$, but the total weight loss in Steps I and II (22.5%) agrees well with the theoretical value (22.7%).

After a prolonged horizontal portion on the weight curve (extending over ca. $200°C$), Step III occurs in the very narrow temperature range of $707-727°C$. The product was white and was confirmed to be Eu_2O_3 from its X-ray crystallogram. The weight loss (5.6%) corresponds to the loss of CO_2 (5.9%). Thus Step III can be represented as follows:

$$Eu_2O_2CO_3 \rightleftarrows Eu_2O_3 + CO_2$$
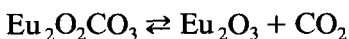
Step III seems to be a reversible process; this is probably the reason why Steps II and III, which overlap in N_2, are well separated in CO_2, in which the reverse reaction is favored.

Dehydration of $Eu_2mal_3 \cdot 6H_2O$

The TG and DTA curves of $Eu_2mal_3 \cdot 6H_2O$ for the runs in N_2, O_2 and CO_2 are shown in Fig. 5. The first step with a weight loss of 14.6% on the TG curve in N_2 corresponds to the loss of $6H_2O$ (15.0%). The corresponding DTA curve is a smooth endotherm with a peak at $153°C$. All the six water molecules in the hydrate are thus lost in a single step. No effect of the ambient atmospheres upon the course of dehydration was observed, as in the case of the oxalate hydrates.

Decomposition of Eu_2mal_3 in N_2

As in the case of Eu_2ox_3, the decomposition of anhydrous Eu_2mal_3 strongly depends on the ambient atmosphere. In N_2, its weight loss begins
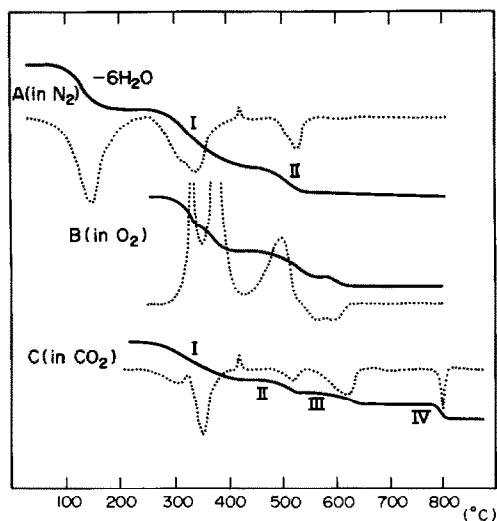
Fig. 5. TG (solid line) and DTA (dotted line) curves of $Eu_2mal_3 \cdot 6H_2O$ in various atmospheres. Heating rates used were $3°C$ min^{-1} for the runs in N_2 and O_2 and $1°$ min^{-1} for the run in CO_2.

at $270°C$ and continues up to $482°C$ (Step I), although the corresponding DTA trace is rather complicated (Fig. 5A). The product after Step I was black and amorphous to X-rays (all the products from the malonate were amorphous, so that X-ray diffraction could not be applied for their identification). Its IR spectrum is very similar to that in Fig. 2A and also to that [10] of $EuCO_3$. The carbon content (11.04%) corresponds to the composition $EuCO_3 + C$ (10.7%), and the observed weight loss (22.8%) is in good agreement with the theoretical value (22.6%) for the product of this composition.

Step II, with a weight loss of 10.4%, occurs in the wide temperature range of $482–790°C$, although most of the weight loss takes place below $550°C$. The product was white, but a considerable amount of elementary carbon was deposited between the white product and the platinum crucible. The observed weight loss is in good agreement with the theoretical value (10.0%) for the loss of CO and CO_2, so that, as for Eu_2ox_3, the final product should be Eu_2O_3 ($+2C$).

Decomposition of Eu_2mal_3 in O_2

In O_2, this compound decomposes through several steps, but none of the weight loss values could be assigned to a distinct product, possibly owing to side reactions. Step I is now separated into two, one at $274–331°C$ ($\Delta W = 10.7\%$) and another at $331–422°C$ ($\Delta W = 9.5\%$), respectively, which are characterized by very large exothermic peaks on the DTA curve (Fig. 5B). Step II is also exothermic. This is certainly due to the combustion of the

evolved gas, which now contains not only CO, but also much hydrogen or hydrogen-rich products (e.g. CH_4), according to the stoichiometries of the possible reactions. In such an oxidizing atmosphere, the formation of Eu(II) is again impeded. $Eu^{III}CH(COO)_2$ may be a possible intermediate formed right after the first stage of Step I, as has been suggested in the thermal decomposition of Na_2mal, K_2mal and Ba(mal) [11]. The observed weight loss (10.7%) of this first stage, however, is much smaller than that for formation of this product (14.5%), suggesting the composite nature of the decomposition.

Decomposition of Eu_2mal_3 in CO_2

In CO_2, this compound decomposes in four steps, instead of the three for the oxalate in the same atmosphere. The initial temperature of the weight–loss is $237°C$, which is considerably lower than those in N_2 ($270°C$) and O_2 ($274°C$), even if the difference in heating rate ($1°$ min^{-1} in CO_2 and $3°$ min^{-1} in N_2 and O_2) is taken into account. The TG curve becomes nearly a plateau at $488°C$ (Step I); the product was yellowish brown, so the amount of elementary carbon in it must be much smaller than in the case of Step I in N_2, but its carbon content was as much as 14.5%. Its IR spectrum (Fig. 6A) is peculiar and apparently different from those of CO_3^{2-} and $-COO^{2-}$. As has been suggested in a previous paper [12], this type of spectrum may be due to $CH(COO)_2^{3-}$, with conjugated C=C bonds. The absorption peak at 1130 cm^{-1} seemingly corresponds to the above bond structure. The high carbon content (14.5%) can also be explained by assuming the formation of
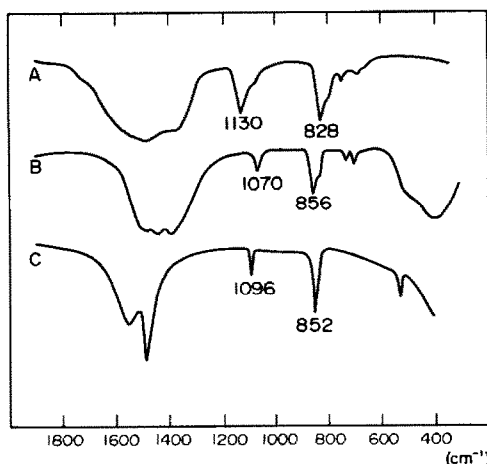

Fig. 6. Infrared spectra of the products immediately after Steps I (A), II (B) and III (C) for Eu_2mal_3 in CO_2.

$EuCH(COO)_2$ (14.2%) at this step. The observed weight loss (18.4%), however, is larger than the expected value (14.5%), so the problem still remains unsolved.

Step II, with a weight loss of 4.0%, occurs in the range 448–552°C. The product was black, indicating the presence of much elementary carbon. Its IR spectrum (Fig. 6B) is generally similar to curve 8, in Fig. 2, which was ascribed to $Eu_2O_2(CO_3)$. Its carbon content was 11.3%, which is near the theoretical value (10.3%) for the composition of $Eu_2O(CO_3)_2 + 2C$. The abundance of elementary carbon in the product seems to support the view that hydrogen is evolved in the course of its formation, producing a fairly reducing atmosphere.

Step III, with weight loss 5.0%, occurs in the range 522–692°C. The product was white, but elementary carbon was deposited separately between it and the platinum crucible. The carbon content in the white product was 4.05%, which is near the theoretical value (3.03%) for $Eu_2O_2CO_3$. The IR spectrum shows the absorptions of both Eu–O and CO_3^{2-} (Fig. 6C), although the positions of the peaks are different from those in Fig. 2B. This spectrum is characterized by the disappearance of the symmetrical stretching band of CO_3^{2-}, which indicates that the CO_3^{2-} is highly symmetrical and suggests that the interaction between Eu^{3+} and CO_3^{2-} is weak. The observed weight loss (5.0%) is near the theoretical value (6.1%) for the loss of CO_2.

The final step (Step IV) occurs in the very narrow temperature range of 772–812°C, as in the case of Step III for the oxalate in the same atmosphere, but the initial temperature (772°C) is much higher than that (707°C) of the oxalate. The weight loss (5.1%) is near the theoretical value (6.1%) for the loss of CO_2. This step can be represented by the same reversible equation as that of Step III for the oxalate in CO_2, but here the reversibility is seemingly higher.

DISCUSSION

Course of dehydration

$Eu_2ox_3 \cdot 10H_2O$ loses its ten water molecules approximately in steps of 4-2-4, whereas $Eu_2mal_3 \cdot 6H_2O$ loses all its water in single step. TG and DTA results seem to reflect the modes of bonding of H_2O in these hydrates. In the light of the X-ray studies of the related compound, $Nd_2(C_2O_4)_3 \cdot 10.5H_2O$ [13], it is probable that four H_2O molecules in the present oxalate are lattice waters, and the remaining six are coordinated to the metal. The TG result shows that the lattice waters are evolved first, then two of the coordinated waters and then the rest. On the other hand, all water molecules in the malonate are equivalently coordinated to the metal atoms [14], and the TG result shows that all of them are evolved equally on heating.

Course of decomposition

The decomposition of the oxalate in N_2 and CO_2 can be essentially described as follows

$$Eu_2ox_3 \xrightarrow{I} Eu^{II}CO_3 \xrightarrow{II} Eu_2^{III}O_2CO_3 \xrightarrow{III} Eu_2O_3$$
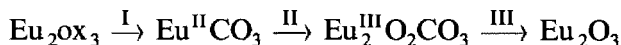
Step I includes the change of Eu(III) to Eu(II). Glasner et al. [1g] have suggested this change, but later Gallagher et al. [1n] put forward a different view (see the introduction). We could confirm the presence of $EuCO_3$ in the product by X-ray diffraction, and all other experimental results also support its formation.

Eu(III) seems to be reduced by CO_2^- which is formed by C–C bond rupture of ox^{2-}. It has been suggested that the decomposition of Na_2ox is initiated by such a bond rupture, and CO_2^- is formed in such systems [15]. Step I is thus probably not simple, and is composed of at least the following three reactions

$$Eu_2^{III}ox_3 \rightarrow \left(Eu_2^{III}ox_2 \cdot 2CO_2^-\right) \rightarrow 2Eu^{II}ox + 2CO_2$$

$$2Euox \rightarrow 2EuCO_3 + C + CO_2$$

$$2Euox \rightarrow 2EuCO_3 + 2CO$$

Euox formed by the first reaction will subsequently decompose to $EuCO_3$ by the second or third reaction. The third reaction becomes more favorable with increasing temperature (Fig. 4A). Formation of elementary carbon has been frequently explained by the disproportionation of evolved CO, but this seems to be improbable in the open system.
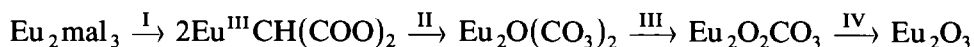
Steps II and III can be represented as follows (respectively)

$$2EuCO_3 \xrightarrow{II} Eu_2^{III}O_2CO_3 + CO$$

$$Eu_2O_2CO_3 \xrightarrow{III} Eu_2O_3 + CO_2$$
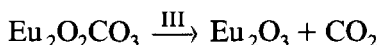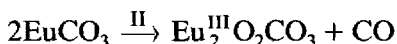
Step II includes the reoxidation of europium, and therefore the onset temperature of Step II seems to depend on the amount of elementary carbon in the product, which as a reductant will suppress this step. In fact, the initial temperature (414°C) of this step for $EuCO_3$ from the oxalate is much lower than that (482°C) for $EuCO_3$ from the malonate. Step II overlaps with Step III in N_2, but both steps are clearly separated in CO_2, because of the reversibility of Step III.

The decomposition of Eu_2mal_3 begins at a lower temperature than that of Eu_2ox_3, and is more strongly affected by the ambient atmosphere. In N_2, its decomposition products are similar to those of the oxalate, except that the products from the malonate are amorphous to X-rays and abound in elementary carbon. In CO_2, however, deprotonation of the $-CH_2-$ group in malonate seems to occur at an early stage of the decomposition, since a

hydrogen atom in the methylene group between two electron-attracting carboxyl groups tends to behave as a proton. The process in CO_2 can be described as follows

$$Eu_2 mal_3 \xrightarrow{\text{I}} 2Eu^{III}CH(COO)_2 \xrightarrow{\text{II}} Eu_2O(CO_3)_2 \xrightarrow{\text{III}} Eu_2O_2CO_3 \xrightarrow{\text{IV}} Eu_2O_3$$

The weight loss values, however, indicate that Steps I and II do not occur stoichiometrically. Probably side reactions such as the Steps I and II in N_2 occur simultaneously.

In conclusion, it can be stated that; (1) in a N_2 atmosphere, the decompositions of the oxalate and malonate are similar, and the reduction of Eu occurs first and then its reoxidation; (2) in a CO_2 atmosphere, however, the decompositions of these salts are apparently different, and a large part of the malonate decomposes without change of the oxidation state of Eu through various intermediates.

REFERENCES

1 (a) W.W. Wendlandt, Anal. Chem., 30 (1958) 58;
   (b) W.W. Wendlandt, Anal. Chem., 31 (1959) 408;
   (c) W.W. Wendlandt, T.D. George and G.R. Horton, J. Inorg. Nucl. Chem., 17 (1961) 273;
   (d) A. Glasner and M. Steinberg, J. Inorg. Nucl. Chem., 16 (1961) 279;
   (e) A. Glasner and M. Steinberg, J. Inorg. Nucl. Chem., 22 (1961) 39;
   (f) A. Glasner and M. Steinberg, J. Inorg. Nucl. Chem., 22 (1961) 156;
   (g) A. Glasner, E. Levy and M. Steinberg, J. Inorg. Nucl. Chem., 25 (1963) 1415;
   (h) V.V.S. Rao, R.V.G. Rao and A.B. Biswas, J. Am. Ceram. Soc., 47 (1964) 356;
   (i) V.V.S. Rao, R.V.G. Rao and A.B. Biswas, J. Inorg. Nucl. Chem., 27 (1965) 2525;
   (j) R. Möbius and F. Matthes, J. Inorg. Nucl. Chem., 28 (1966) 1601;
   (k) R. Möbius, W. Dietzold and F. Matthes, J. Inorg. Nucl. Chem., 28 (1966) 1847;
   (l) R.P. Turcotte, J.O. Sawyer and L. Eyring, Inorg. Chem., 8 (1969) 238;
   (m) K.G. Nair, V.V. Sreerajan and V.S.V. Nayar, Thermochim. Acta, 39 (1980) 253;
   (n) P.K. Gallagher, F. Schrey and B. Prescott, Inorg. Chem., 9 (1970) 215;
   (o) M.J. Fuller and J. Pinkstone, J. Less-Common Met., 70 (1980) 127;
   (p) A. Kahwa and A.M. Mulokozi, J. Therm. Anal., 22 (1981) 61;
   (q) Yu.A. Ageev, I.R. Nevskii, V.G. Mizin, S.A. Archugov and G.I. Kazanets, Russ. J. Inorg. Chem., 27 (1982) 1573;
   (r) G.L. Jeyaraj and J.E. House, Jr., Thermochim. Acta, 71 (1983) 345.
2 B.S. Azikov and V.V. Serebrennikov, Zh. Neorg. Khim., 12 (1967) 445.
3 H.N. McCoy, J. Am. Chem. Soc., 61 (1939) 245.
4 K. Nagase, Bull. Chem. Soc. Jpn., 46 (1973) 144.
5 Joint Committee on Powder Diffraction Standards, Inorg. Vol., 17-309.
6 W.E. Brown, D. Dollimore and A.K. Galwey, in C.H. Bamford and C.F.H. Tipper (Eds.), Comprehensive Chemical Kinetics, Vol. 22, Reaction in the Solid State, Elsevier, Amsterdam, 1980, p. 208.
7 (a) H.J.T. Ellingham, J. Soc. Chem. Ind., 63 (1944) 125;
   (b) J.D. Lee, A New Concise Inorganic Chemistry, Van Nostrand–Reinhold, Berkshire, 1977, Chap. 3.

8 (a) N.T. McDevitt and W.L. Baun, Spectrochim. Acta, 20 (1964) 799;
  (b) F.F. Bentley, L.D. Smithson and A.L. Rozek, Infrared Spectra and Characteristic Frequencies—700–300 cm^{-1}, Interscience, New York, 1967, p. 101.
9 M. Shyamala, S.R. Dharwadkar and M.S. Chandrasekharaiah, Thermochim. Acta, 56 (1982) 135.
10 A. Glasner, E. Levy, M. Steinberg and W. Bodenheimer, Talanta, 11 (1964) 405.
11 S. Shishido and K. Ogasawara, Sci. Rep. Niigata Univ., Ser. C, 3 (1971) 23.
12 K. Muraishi, K. Nagase and N. Tanaka, Thermochim. Acta, 23 (1978) 125.
13 E. Hasson, Acta Chem. Scand., 24 (1970) 2969.
14 E. Hasson, Acta Chem. Scand., 27 (1973) 2813.
15 K.O. Hartman and I.C. Hisatsune, J. Phys. Chem., 71 (1967) 392.